

Theor Appl Climatol (2011) 105:167–180  
DOI 10.1007/s00704-010-0381-9

ORIGINAL PAPER

# Five centuries of Southern Moravian drought variations revealed from living and historic tree rings

Ulf Büntgen · Rudolf Brázdil · Petr Dobrovolný ·  
Mirek Trnka · Tomáš Kyncl

Received: 8 September 2010 / Accepted: 1 December 2010 / Published online: 21 December 2010  
© Springer-Verlag 2010

**Abstract** Past, present, and projected fluctuations of the hydrological cycle, associated to anthropogenic climate change, describe a pending challenge for natural ecosystems and human civilizations. Here, we compile and analyze long meteorological records from Brno, Czech Republic and nearby tree-ring measurements of living and historic firs from Southern Moravia. This unique paleoclimatic compilation together with innovative reconstruction methods and error estimates allows regional-scale May–June drought variability to be estimated back to AD 1500. Driest and wettest conditions occurred in 1653 and 1713, respectively. The ten wettest decades are evenly distributed throughout time, whereas the driest episodes occurred in the seventeenth century and from the 1840s onward. Discussion emphasizes agreement between the new reconstruction and documentary evidence, and stresses possible sources of reconstruction uncertainty including station inhomogeneity, limited frequen-

cy preservation, reduced climate sensitivity, and large-scale constraints.

## 1 Introduction

Precipitation is the most important meteorological driver of ecosystem functioning, agricultural productivity, and societal prosperity (IPCC 2007). A detailed understanding of past, present, and projected changes in the hydrological cycle (Huntington 2006), particularly in continental regions where summer precipitation totals may significantly vary on interannual to multidecadal timescales, and thus possibly constrain economic wealth and human health (e.g., Cook et al. 2007), describes a critical research task for the interdisciplinary climate change community.

Shifts in water availability may become exceptionally important for Central Europe (Pauling et al. 2006), including the Czech Republic watersheds, from which the continent's major rivers originate: the Elbe (from Bohemia), and the Oder and Morava (both from Moravia), with the latter being a tributary of the Danube. A predicted increase in drought frequency and severity is expected to alter significantly water management (e.g., Brázdil et al. 2009), as well as forest productivity and agricultural economy. A detailed understanding of temporal changes in precipitation totals on timescale longer than decades (Büntgen et al. 2010a, c), as well as of complex spatial regime shifts (Büntgen et al. 2010b), is important not only for climatologists, ecologists, and biologists but also for economists and politicians, ensuring a sustainable organization of future water (re)sources. Enhanced knowledge of past (natural) hydroclimatic variability will put recent political and fiscal reluctance to adapt to and mitigate projected (anthropogenic) climate change into perspective (IPCC 2007).

---

U. Büntgen (✉)  
Swiss Federal Research Institute WSL,  
8903 Birmensdorf, Switzerland  
e-mail: [buentgen@wsl.ch](mailto:buentgen@wsl.ch)  
URL: [www.buentgen.com](http://www.buentgen.com)

U. Büntgen  
Oeschger Centre for Climate Change Research,  
3012 Bern, Switzerland

R. Brázdil · P. Dobrovolný  
Institute of Geography, Masaryk University,  
61137 Brno, Czech Republic

M. Trnka  
Institute of Agrosystems and Bioclimatology, Mendel University,  
61300 Brno, Czech Republic

T. Kyncl  
Moravian Dendro-Labor,  
61600 Brno, Czech Republic

The longest precipitation series in Europe originate from France and England where precipitation measurements started as early as the 1680s in Paris (Slonosky 2002) and where continuous observations reach back to 1697 in Kew (Wales-Smith 1971). Nevertheless, systematic measurements in most of the continent's cities started not before the nineteenth century (Auer et al. 2007). The first meteorological station in the Czech Lands was launched in the winter of 1719/1720 (Zákupy, northwestern Bohemia). Continuous precipitation measurements from the eighteenth century are, however, fairly rare, and systematic precipitation measurements started in Brno 1803 and 1 year later at the Klementinum in Prague. The number of rain gauge stations in the Czech Lands significantly increased in the second half of the nineteenth century. Station relocations, as well as differently utilized types and heights of rain gauges, however, often biased such long measurement series, and proper homogenization procedures remain challenging (Auer et al. 2007). The employment of annually resolved man-made and natural proxy data (e.g., documentary archives and tree rings) or their combination describes a unique way of extending instrumental station records back in time (e.g., Brázdil et al. 2005, 2010; Büntgen et al. 2005; Moberg et al. 2005; Dobrovolný et al. 2010), and even allows early instrumental biases to be assessed (Frank et al. 2007a).

Here, we revisit meteorological station measurements from the Brno territory back to AD 1803 and tree-ring width (TRW) measurements from living and historic firs (*Abies alba* Mill.) from Southern Moravia back to AD 1325. We present a new reconstruction of regional-scale May–June (MJ) interannual to multidecadal drought variability back to AD 1500, which is surrounded by error bars and compared with documentary archives.

## 2 Data, methods, and results

Monthly resolved precipitation and temperature data from Brno, which started in January 1803 and have been homogenized in the framework of the HISTALP project (Auer et al. 2007), were herein used for the calculation of the Palmer Drought Severity Index (PDSI) and the Z-index (ZIND). The PDSI has been demonstrated to represent sufficiently prolonged episodes of soil moisture deficit as reflected by different tree-ring chronologies (e.g., Cook et al. 2007; Esper et al. 2007; Büntgen et al. 2010a, b, c). The PDSI is based on the supply-and-demand concept of water balance; incorporates antecedent precipitation, moisture supply, and demand at the surface; and follows the calculation method introduced by Thornthwaite (1948). The PDSI applies a two-layer bucket-type model for soil moisture computations with three assumptions of different soil profile characteristics: The water holding capacity of

the surface layer ( $S_s$ ) is set to a maximum of 25 mm, the water holding capacity of the underlying layer ( $S_u$ ) has a maximum value dependent on the soil type, and water transfer into or out of the lower layer solely occurs when the surface layer is full or empty, respectively. The PDSI therefore describes an accumulative departure relative to local mean conditions in atmospheric surface moisture supply and demand (Palmer 1965). The PDSI well represents prolonged episodes of drought. The PDSI estimate includes an intermediate step, known as the Palmer Moisture Anomaly Index (or ZIND), which is a measure of surface moisture anomaly for a current month without consideration of the antecedent conditions that are so characteristic for the PDSI. It basically represents the moisture departure, adjusted by a weighting factor of climatic characteristic. The ZIND can therefore be used to better track short-term seasonal droughts as it responds more direct to changes in soil moisture (Karl 1986). We herein used the so-called self-calibrated version (Wells et al. 2004) of the ZIND and PDSI. Wells et al. (2004) modified the original Palmer model in order to adjust the former empirical constants automatically according to the input data uniquely derived from each of the studied locations. A simple snow-accumulation and snowmelt model was further implemented to account for the occurrence of snow (van der Schrier et al. 2007). Model simulations started 10 years prior to the initial date of the given series using monthly temperature and precipitation means. The first 24 months of the drought metric were excluded to avoid misinterpretations during the spin-up interval. The water holding capacity was derived from the national soil survey and herein confronted with data from Webb et al. (1993). Given the uncertainty in properly estimating this parameter at our sampling sites, a sensitivity analysis that compared PDSI and ZIND values across the whole range of plausible values (160 to 360 mm) was performed. A single value of 260 mm was used for the whole period under consideration and for all drought index calculations. This suite includes 12 grid-boxes between 15°40' and 16°10' E and 48°50' to 49°10' N, with an altitudinal range of 201–505 m asl. High-resolution 10'×10' precipitation, temperature, and drought grids kindly provided by the Climatic Research Unit (CRU; Mitchell et al. 2004; <http://www.cru.uea.ac.uk/~timm/data/index-table.html>) were employed to explore the spatial signature of MJ precipitation and drought variability of the fir-sampling region.

A total of 117 living and 165 historic fir TRW samples from Southern Moravia (mainly south of the city of Brno) were compiled (Figs. 1b and 2a). Replication is decreasing back in time, and the period before AD 1500, during which sample size partly drops below 10 series, remains unreliable for climate reconstruction purposes. Growth trends and levels within the raw TRW measurements were evaluated

**Fig. 1** **A** European perspective on 13 (annually resolved) hydroclimatic (precipitation/drought) reconstructions used for comparison (see Table 2 for further details). **B** Location of the living and historic TRW sites, and the Brno meteorological station used

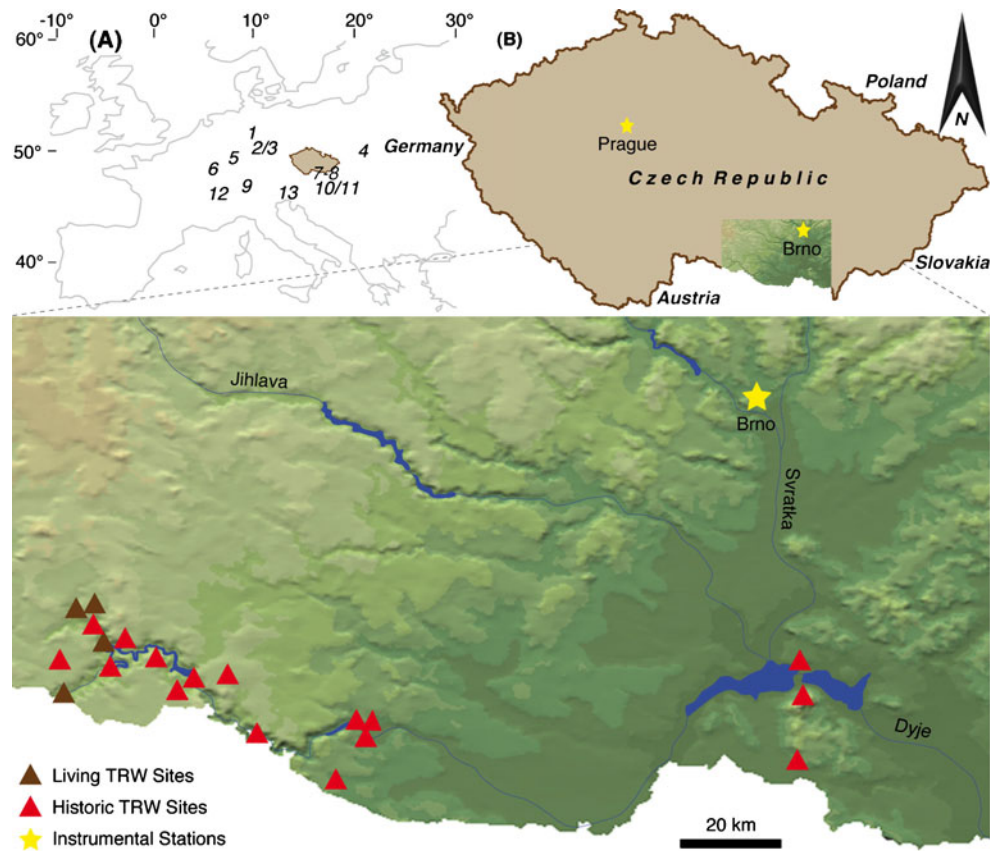
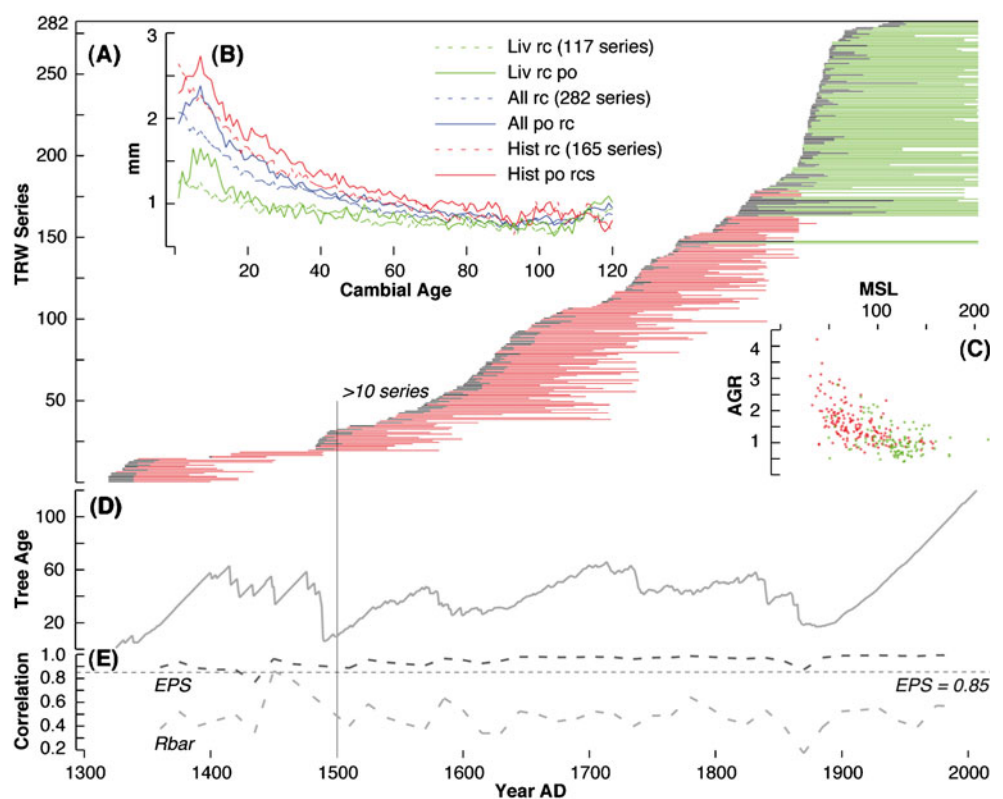


**Fig. 2** **A** Temporal distribution of the 117 living (*Liv*; green) and 165 historic (*Hist*; red) TRW series, and their corresponding pith-offset (*po*; gray). **B** Regional curves (RCs) of the data mean (*All*; 282 series) and the subsets (*Liv* and *Hist*) with and without considering pith-offset (*po*). **C** Relationship between mean segment length (*MSL*) and average growth rate (*AGR*) classified into living and historic data. *MSL* and *AGR* of all 282 series are 95 years and 1.37 mm with only small differences between the living (116 years and 1.08 mm) and historic (79 years and 1.57 mm) subsets. **D** Mean tree age, as well as **(E)** EPS and *Rbar* statistics



after age-aligning the individual series by their innermost ring, preferentially their cambial age (Fig. 2b). The mean of the age-aligned series, the so-called regional curve (RC), describes the common growth trend and level at a given tree age, resembling a negative exponential function. A clear link between segment length and average ring width is obtained for each series (Fig. 2c). The temporal evolution of the mean tree age of the dataset indicates fairly constant values of ~60 years for most of the dataset (Fig. 2d), whereas mean tree age increases up to 120 years by the end of the twentieth century. The expressed population signal (EPS) and the interseries correlation (Rbar), calculated over 30 years lagged by 15 years (Wigley et al. 1984), reveal robust signal strength along the living and historic samples back into the fourteenth century (Fig. 2e). Mean EPS and Rbar values are 0.95 and 0.48, respectively, computed over the full record length.

To remove nonclimatic, biological-induced growth trends (so-called age trends as visualized by the RCs) from the raw TRW measurements, and to test for possible influences of age-trend removal on low-frequency preservation and the associated skill of recent tree growth to track hydroclimatic variability, different detrending techniques were applied: 150- and 300-year cubic smoothing splines with 50% frequency response cutoff at 150 and 300 years (SPL), negative exponential functions (NEF), and the regional curve standardization (RCS; Esper et al. 2003). These methods were chosen as they denote standard techniques used for growth–climate response analyses and climate reconstructions, known to retain high- to low-frequency information. To further account for possible end-effect biases associated with the chronology development process, two different techniques of index calculation were utilized: Ratios or residuals after power transformation (PT) were calculated between the original measurements and their corresponding growth fits (Cook and Peters 1997). Pith-offset estimates were considered for a correct treatment of the RCS method. Mean chronologies were calculated using a biweight robust mean, their variance stabilized (Frank et al. 2007b), and records truncated at a minimum replication of 10 series. Given the age structure of the fir data compiled and the methodological constraints of the detrending applied (Cook and Peters 1981; Esper et al. 2003), we expect the SPL detrending, followed by NEF and RCS to most alter the low-frequency spectra of the resulting time series, whereas the retained higher frequency, interannual to multidecadal variability, would generally remain unaffected (Büntgen et al. 2008). The different detrending techniques were consecutively applied to the living, historic, and combined datasets (Büntgen et al. 2005). Moreover, wavelet analysis (Torrence and Compo 1998) was used to compare typical features in frequency spectra and behavior of the instrumental target and tree-ring proxy records.

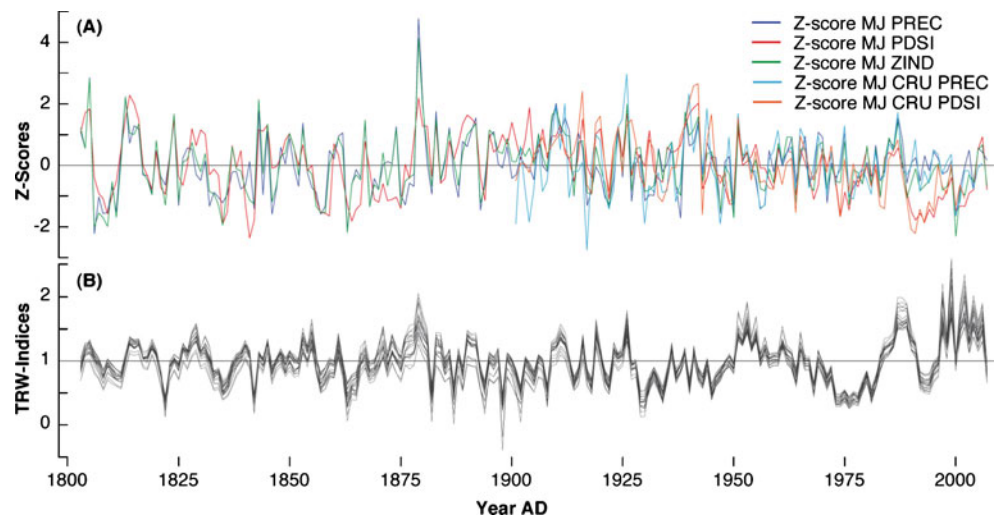
Correlation coefficients were computed between the different TRW chronologies and the instrumental-based precipitation, ZIND, and PDSI records using different split periods (Fig. 4). Mean and variance of the proxy data were finally scaled to the corresponding target values over the 1803–1932 period. This calibration procedure is the simplest among various techniques though perhaps least prone to variance underestimation. The estimated error bars include effects of the tree-ring data used (horizontal splitting) and the detrending techniques applied (SPL, NEF, RCS with and without PT), as well as the root mean squared error (RMSE) of the calibration period (see Esper et al. 2007 for methodological details).

Comparison between the monthly resolved precipitation, ZIND and PDSI indices, and different TRW chronologies reveals similar as well as different behavior throughout the past two centuries (Fig. 3). Time series of both the hydroclimatic targets and the TRW proxies show interannual to multidecadal fluctuations, whereas significant longer-term trends are generally missing. The target data indicate slightly drier conditions before around 1880 and after 1950. A pronounced growth depression in the TRW data occurred in the 1930s and 1940s, as well as in the 1970s. A distinct growth increase during the last decade contradicts negative drought anomalies. Correlations between the different TRW chronologies and the various climatic indices describe nonsignificant influences of previous year climate on radial growth (not shown). Correlations are generally positive for the current year spring/summer months between April and September, and highest correlations are found with MJ (Fig. 4). Differences between the three meteorological variables and fir growth are evident, though in line with the different first order autocorrelation structures (precipitation=0.06, ZIND=0.18, PDSI=0.56). While the response patterns are fairly similar for precipitation and ZIND (Fig. 4a, b), a more persistent response behavior is found with the PDSI (Fig. 4c). This overall picture appears to be stable when using early/late (1803–1905/1905–2007) split periods. Most interesting is the significant loss of hydroclimatic sensitivity of fir growth during the second split interval. Highest correlations between fir growth and all three hydroclimatic elements are obtained when using MJ variations of the early window (0.52–0.54), whereas highest values of the late period only range in the order of 0.33–0.39. Smallest though pronounced temporal response changes are obvious for the ZIND data. Effects of the different detrending (SPL, NEF, RCS with and without PT) and chronology development (horizontal splitting) techniques are trifling and do not influence the achieved growth–climate response relationships.

Running 21-year correlation coefficients between measured and reconstructed MJ ZIND are fairly stable over the 1803–1932 calibration period, although they tend to



**Fig. 3** **A** Instrumental-based precipitation, PDSI and ZIND calculated from the Brno station (1803–2008) and the CRU (1901–2002). **B** Common fir TRW variability of the slightly different chronologies after various detrending and chronology development techniques



slightly decrease back in time (Fig. 5a). The new MJ ZIND reconstruction captures interannual to decadal-scale variability (Fig. 5b). The MJ conditions of 1879 describe the wettest extreme common to the proxy and target data. Overall, wetter summers in the 1880s were followed by a shift toward generally drier conditions until present. Nevertheless, significant hydroclimatic long-term changes during the calibration period were not observable, neither in the target nor the proxy time series. The MJ ZIND reconstruction illustrates fairly dry conditions in the early seventeenth century (Fig. 5c). Extremely wet conditions occurred in 1713, 1649, and 1879, whereas the driest years were 1653, 1636, and 1898. Decadal-scale and longer fluctuations have not been observed, despite the tendency towards a slightly drier twentieth century.

Frequency-dependent behavior of the measured and reconstructed Southern Moravian MJ ZIND demonstrates spectral differences between both series (Fig. 6). The global wavelets show significant periodicity between 16 and

32 years for the measured data and between 8 and 64 years for the reconstructed data.

### 3 Discussion and conclusions

Comparison of the 20 highest and lowest values of the reconstructed MJ ZIND between 1500 and 1932 with monthly ZIND indices and precipitation totals of the April to July interval from the Brno station back to 1803 and documentary evidence from the Czech Lands back to 1500 (e.g., Brázdil et al. 2005) demonstrates reasonable agreement (Table 1). Most of the detected negative ZIND values (dry periods) occurred in the seventeenth and nineteenth century (6 years each), whereas most of the positive ZIND values (wet periods) date into the eighteenth century. The first phase of wet events clustered from 1712 to 1714 with the occurrence of severe floods in every year. The second cluster from 1769 to 1772, known as “hungry years”

**Fig. 4** Correlation coefficients between 24 slightly different TRW chronologies (using all data and the combined living/historic subsets), as well as instrumental-based (A) precipitation, (B) ZIND, and (C) PDSI computed over two early/late split intervals (1803–1905/1905–2007) and the full period (1803–2007) of proxy–target overlap. Only correlation coefficients  $>0.25$  and using monthly growing season means between April and September and 15 associated seasonal means are shown. The gray vertical shadings denote the MJ period of maximum response

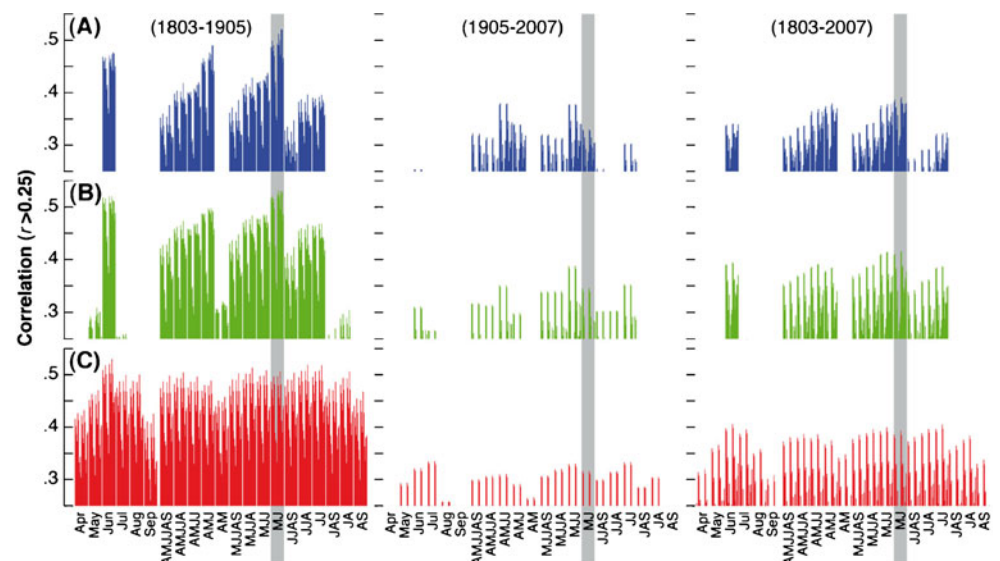
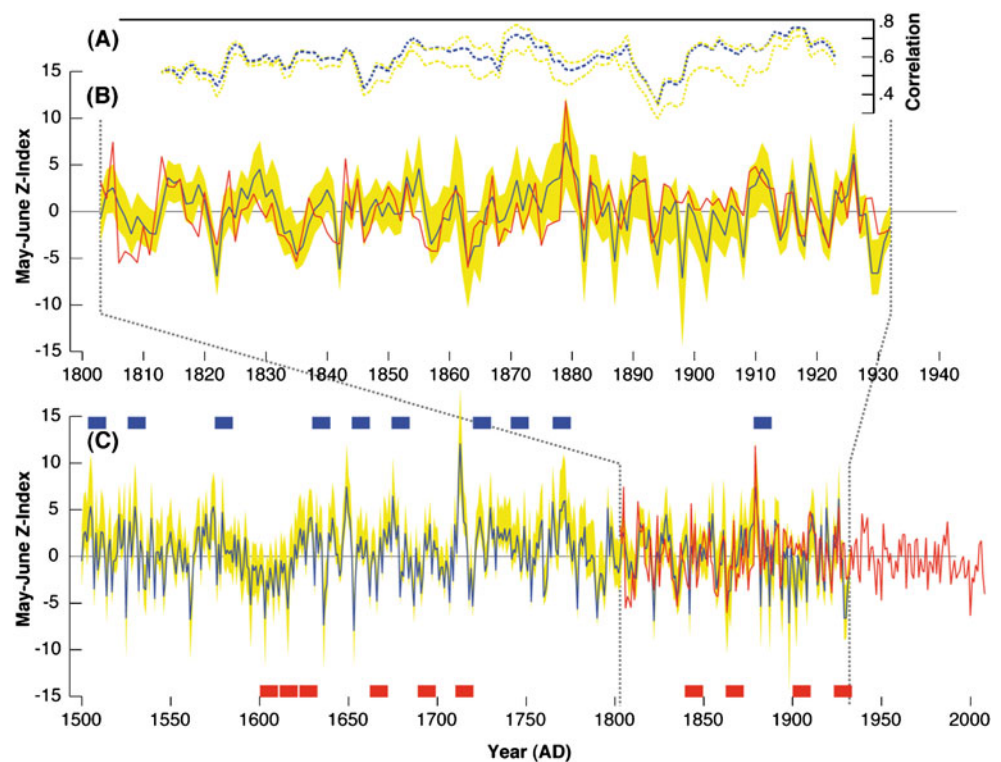


**Fig. 5** **A** Twenty-one-year running correlations between the min/max (yellow) and mean (blue) TRW chronologies and the Brno MJ ZIND computed over the 1803–1932 calibration period. **B** Modeled (blue) and measured (red) ZIND within its estimated uncertainty range (yellow), and **(C)** the full 1500–2008 period of the calculated and reconstructed ZIND with the boxes referring to the ten wettest (blue) and ten driest (red) decades



(Pfister and Brázdil 2006), was characterized by very bad crop harvest followed by dearth, hunger, and high mortality due to epidemic disease in Bohemia where 1/10 of the population died. This period was associated with one of the most rigorous demographic crises in the Czech Lands over the past millennium with far-ranging socioeconomic consequences (Pfister and Brázdil 2006).

Station measurements, particularly when spanning long time periods and thus reaching well back into the

nineteenth century prior to the first meteorological conference in Vienna AD 1893 (e.g., Auer et al. 2007; Frank et al. 2007a), most likely contain nonclimatic noise caused by station relocations, instrumental replacements, and their operating systems, changes in recording times and observers, algorithms for the calculation of means, and other site-specific modifications (e.g., Frank et al. 2007a). Impacts arising from the above concert often occur randomly distributed in time and direction, and therefore call for a comprehensive

**Fig. 6** Wavelet power spectrum (left) of the (A) reconstructed (1500–1932) and (B) measured (1803–2008) MJ ZIND time series. The hatched parts are under the cone of influence and therefore less reliable. The black line is the 10% significance level, using a red-noise (autoregressive lag-1) background spectrum as null hypothesis. The power has been scaled by the global wavelet spectrum (right). The dashed lines are the significance levels for the global wavelet spectra assuming the same significance level and background spectrum as for the corresponding power spectra

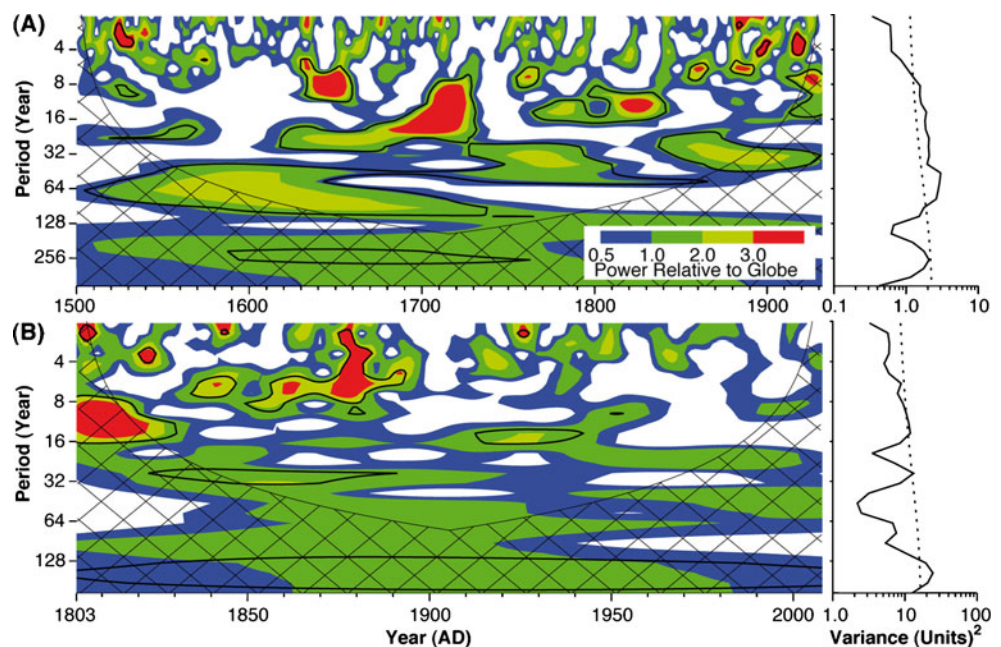


**Table 1** The 20 most negative (A) and positive (B) TRW-based ZIND values (1501–1932) for Southern Moravia in comparison with precipitation totals and calculated ZIND values (monthly precipitation totals from April–July of Brno during the instrumental period are expressed in percentage of the corresponding 1961–1990 reference period) and documentary evidence

Year	Z-index	Short description of weather or related events and comparison with measurements
<b>A</b>		
1653	-7.96	Dry April and May
1636	-7.36	Moderately dry year (dry September and October 1635)
1898	-7.14	Brno: April 165.1%, May 116.3%, June 74.9%, July 108.2%, ZIND=0.92
1822	-6.94	Brno: April 79.4%, May 103.2%, June 49.9%, July 111.3%, ZIND=-3.61
1561	-6.78	Very dry summer (severe winter 1560–1561)
1603	-6.67	Great drought, from spring to harvest no rains
1790	-6.64	Drought from March to June (processions for water, brooks dried up, bad spring cereals)
1525	-6.62	Hot and dry summer
1930	-6.61	Brno: April 149.2%, May 77.0%, June 38.8%, July 106.6%, ZIND=-2.45
1929	-6.61	Brno: April 54.0%, May 157.3%, June 69.3%, July 128.5%, ZIND=1.45 (severe winter 1928–1929)
1842	-6.21	Brno: April 57.1%, May 42.6%, June 51.3%, July 89.3%, ZIND=-3.52
1863	-5.87	Brno: April 92.1%, May 31.1%, June 15.2%, July 11.0%, ZIND=-6.02
1779	-5.67	Drought from spring to mid-June (less water in rivers—mills out of operation)
1616	-5.62	Drought from April to August
1902	-5.45	Brno: April 41.3%, May 44.2%, June 159.4%, July 87.8%, ZIND=1.44
1882	-5.37	Brno: April 95.2%, May 70.5, June 58.2%, July 133.2%, ZIND=-2.01
1887	-5.35	Brno: April 63.5%, May 160.6%, June 22.2%, July 59.6%, ZIND=0.31
1720	-5.36	Great drought (on 8 May a beseeching procession for water)
1687	-5.34	Drought in spring and summer
1595	-5.21	Bad harvest due to heat and drought (dry summer 1594; severe winter 1594–1595)
<b>B</b>		
1713	12.10	Wet year, frequent rains. Floods in March, June, and August
1712	8.14	Wet April (floods)
1649	7.47	No contemporary interpretable report of precipitation patterns in May–July
1879	7.43	Brno: April 200.0%, May 168.8%, June 381.2%, July 112.9%, ZIND=11.84. Floods in June
1714	7.36	Wet June and July, floods in July, bad wine due to wet patterns
1675	6.48	Wet summer, floods in June
1926	6.18	Brno: April 66.7%, May 137.6%, June 191.3%, July 133.2%, ZIND=5.27. Floods in June
1772	6.00	Dry May and normal June (mild winter 1771–1772)
1765	5.87	Wet June
1771	5.83	Very wet summer. Floods in March, April, and June
1574	5.36	No contemporary interpretable reports in terms of precipitation patterns
1505	5.36	Floods in July, grain rotted due to wet patterns (mild winter 1504–1505)
1530	5.35	No contemporary interpretable reports in terms of precipitation patterns
1730	5.25	Very wet summer
1796	5.22	Wet June
1919	5.22	Brno: April 136.5%, May 60.6%, June 124.8%, July 164.6%, ZIND=1.52. Floods in July
1769	5.02	Wet summer. Floods in August
1880	4.89	Brno: April 98.4%, May 280.2%, June 74.9%, July 116.0%, ZIND=5.02. Floods in May, June, August
1770	4.83	Wet summer. Floods in August
1579	4.74	Wet summer. Floods in June

homogenization *modus operandi*. The availability of reliable and continuous metadata and their accurate interpretation, however, display a fundamental task at the forefront of climatology. As for precipitation measurements, the exis-

tence of systematic errors in observational time series represents a separated problem. Such errors, depending on the type of rain gauge used, as well as its installation system and recording interval, are further complicated by external

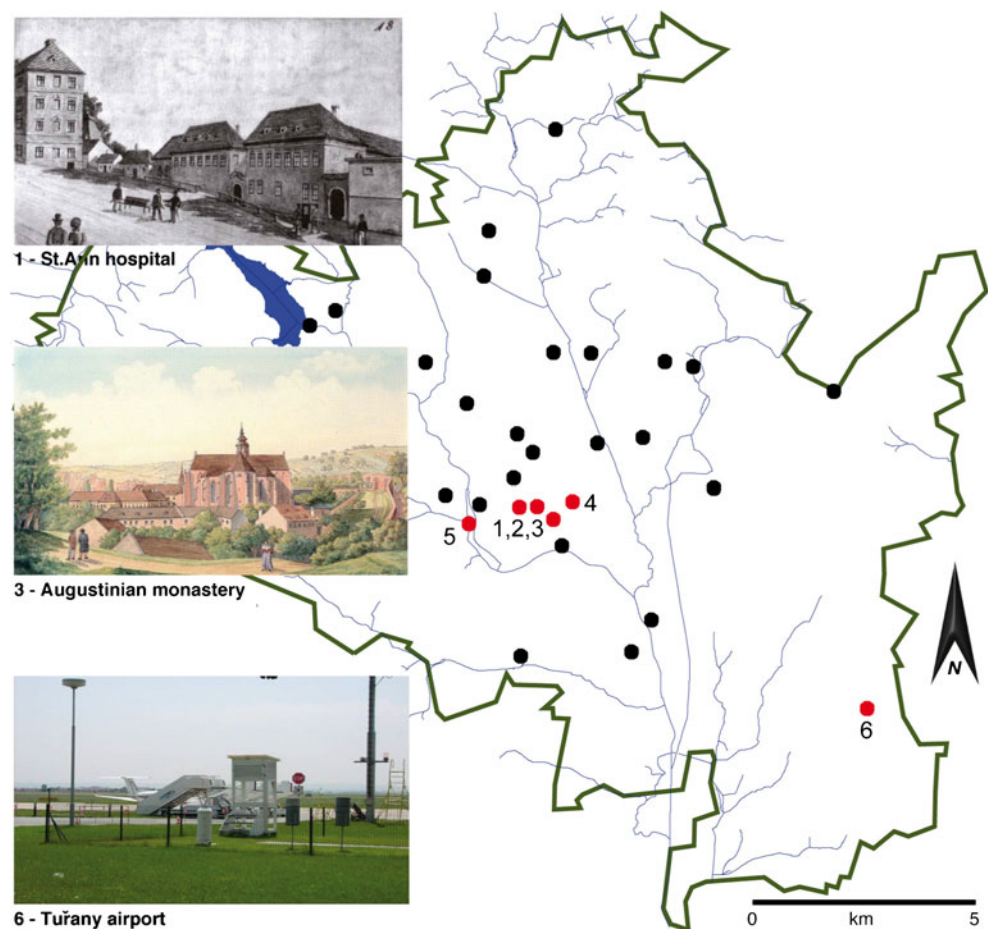


wind disturbances (aerodynamic effect), evaporation of rain water, and wetting of measurement device, with all of them likely causing artificially diminished measurement totals. This situation complicates any homogenization procedure, and the resulting precipitation series may therefore contain some degree of error. Figure 7 provides an overview of the various station locations within the Brno territory and during the past two centuries. In spite of the fact that precipitation measurements—especially before 1890—were performed at several different places within the town, all measurements have been recalculated to the position of the (actual) reference station at the Tuřany airport and homogenized (Auer et al. 2007).

Statistical removal of the biological age trend while simultaneously retaining relevant environmental, e.g., climatic information describes a challenging task (see references herein). Associated methodological constraints are particularly demanding when external long-term trends, such as drying conditions parallel the age trend. Nevertheless, standardization/detrending of the raw data with the overall aim to preserve as much high- to low-frequency information as possible prior to any meaningful interpretation is necessary. The application of rather inflexible cubic smoothing splines can maintain low-frequency variance, and utilization of the RCS method might

even allow variations on time scales longer than the individual segment length to be preserved (Cook et al. 1995). It should be noted that documentary evidence based upon personal accounts of weather extremes is also constrained to a fraction of individual lifespan and thus appears to be limited when trying to reconstruct any long-term changes (Brázdil et al. 2010; Dobrovolný et al. 2010). Compilation of many short documentary series very likely implies problems analogous to those described for tree-ring data as the “segment length curse” (Cook et al. 1995). While tree-ring detrending approaches may help to overcome possible limitations of trend preservation, the RCS method is, however, known to be particularly error prone (e.g., Esper et al. 2003; Büntgen et al. 2005). Their sensitivity to low sample replication, common age structure, and systematic end-effect bias should not be ignored. Resulting values were herein solely employed to enter the error range of the final chronology. On the opposite of the spectrum also appear limitations, because prewhitened TRW chronologies for which the autocorrelative structure has been removed most likely contain too much high-frequency variance. On the other hand, biological autocorrelation that is a characteristic feature of tree-ring (Frank et al. 2007b) and other proxy data (Moberg et al. 2005) may imply too much memory, with the resulting

**Fig. 7** Spatial distribution of meteorological stations with precipitation measurements within the Brno territory (green) throughout the past two centuries. Red circles refer to those stations that have been used in the final precipitation series herein considered: 1 St. Ann hospital (1848–1853), 2 Pekařská street (1853–1858), 3 Augustinian Monastery (1878–1883), 4 German Technical University (1884–1890), 5 Pisárky (1890–1958), and 6 Tuřany airport (1958–present)



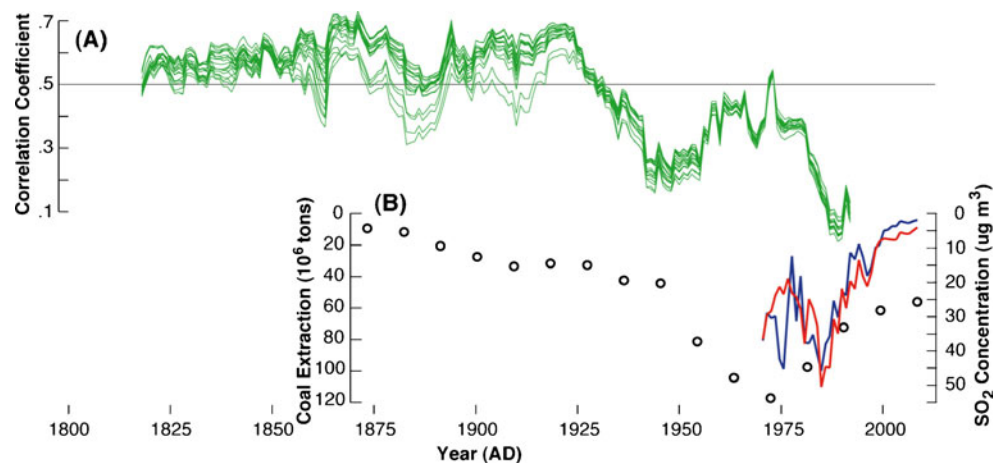


reconstructions contain too much low-frequency variance. Calibration exercises that separately process high- and low-frequency components (Büntgen et al. 2005) may describe a useful approach to overcome some of these spectral color-issues. It should further be considered that the preservation and appropriate weighting of different frequency domains are a critical task for most if not to all existing studies (Moberg et al. 2005), and thus not only describe a problem that is restricted to TRW data. A critical issue common to most paleoclimatic records is also the assessment of a reliable variance stabilization method, which is robust enough to account for artificial changes in interannual variability over time (Frank et al. 2007b).

Temporal instability in the growth–climate relationship has been broadly discussed and might include statistical uncertainty due to the calibration methods applied, biological persistence in the TRW data, nonlinear growth–climate responses, reduction of station measurements back in time, and their different homogenization adjustments, as well as age-related physiological mechanisms, i.e., our chronology contains an extraordinary high mean tree age during the second half of the twentieth century, which implies age/size-related changes in water uptake, as older and larger trees are less sensitive to soil moisture deficits than younger and smaller trees. “Fir dying” might be an additional factor to be herein considered (Vrška et al. 2009). It was originally associated with human activity, but it may be influenced by various other stressors including small resistance to sudden site changes, air pollution, acid rain-releasing free ions of Al and Mn in the soil, climatic extremes, warming and drying of the landscape, draining of stands, disorders in water operation, insect calamities, fungus diseases, epidemic virus diseases, game over breeding, and half-parasitic mistletoe, as well as their complex interactions and insufficient genetic variability resulting in a weak total adaptation capability. The above mentioned stressors should contribute to the significant distortion of relations between precipitation and fir growth in the 1930s (Fig. 8a). Radial fir growth was

already impacted by severe winter conditions in 1928/1929, followed by a sequence of very cold winters in the early 1940s. Harsh frosts of those winters damaged fir trees across Southern Moravia. Most of the fir samples herein compiled showed significant growth reductions with partly missing rings in 1929, as well as distinct signs of chronicle damage including strong defoliation and secondary branching. Traumatic resin channels, probably related to cambium damage, were also found. Similar patterns have been reported for other sites and species across Central–East Europe (W. Tegel, R. Kaczka, and T. Wazny, personal communication). The turn of the 1920s to 1930s was characterized by a sudden increase in mean summer and autumn temperatures (more than 1°C), terminating an overall cooler period that started in the 1830s (Dobrovolný et al. 2009). A sequence of drought events in the first half of the 1930s, together with a prolonged drought episode between 1947 and 1954, was additionally impacting radial growth across most of the continent’s temperate forests (Friedrichs et al. 2009a, b). A slow though continuous drying trend over the twentieth century culminated in two distinct drought episodes from 1988 to 1994 and from 2000 onward. Drought effects on TRW have been further amplified after the 1980s by increasing summer half-year temperatures (Brázdil et al. 2009). Human impact including airborne pollution (Fig. 8b) must be further considered as a negative stressor of tree growth, particularly since Central Europe belongs to one of the most industrialized parts of the world (IPCC 2007). In light of the twentieth century, the world economic crisis of the 1930s was followed in its second part by armament for the Second World War in Central Europe with great development of heavy and machine industry contributing to increasing air pollution and acid rains. Industrialization continued by a postwar restoration, and after 1948, Czechoslovakia became a center for heavy industry within the eastern European countries, indicated by increasing regional coal extraction (Fig. 8b). Coal was a key source for energy production in local power plants and industrial centers. Besides the economic crises in the 1930s, the extraction

**Fig. 8** **A** Twenty-one-year running correlation coefficients between 24 slightly different fir TRW chronologies and the Brno MJ ZIND record. **B** Development of coal extraction in the Czech Republic (1876–2008) and SO<sub>2</sub> concentrations measured at the Brno stations (1971–2008): Kroftova street (urban; blue), Tuřany airport (rural; red)



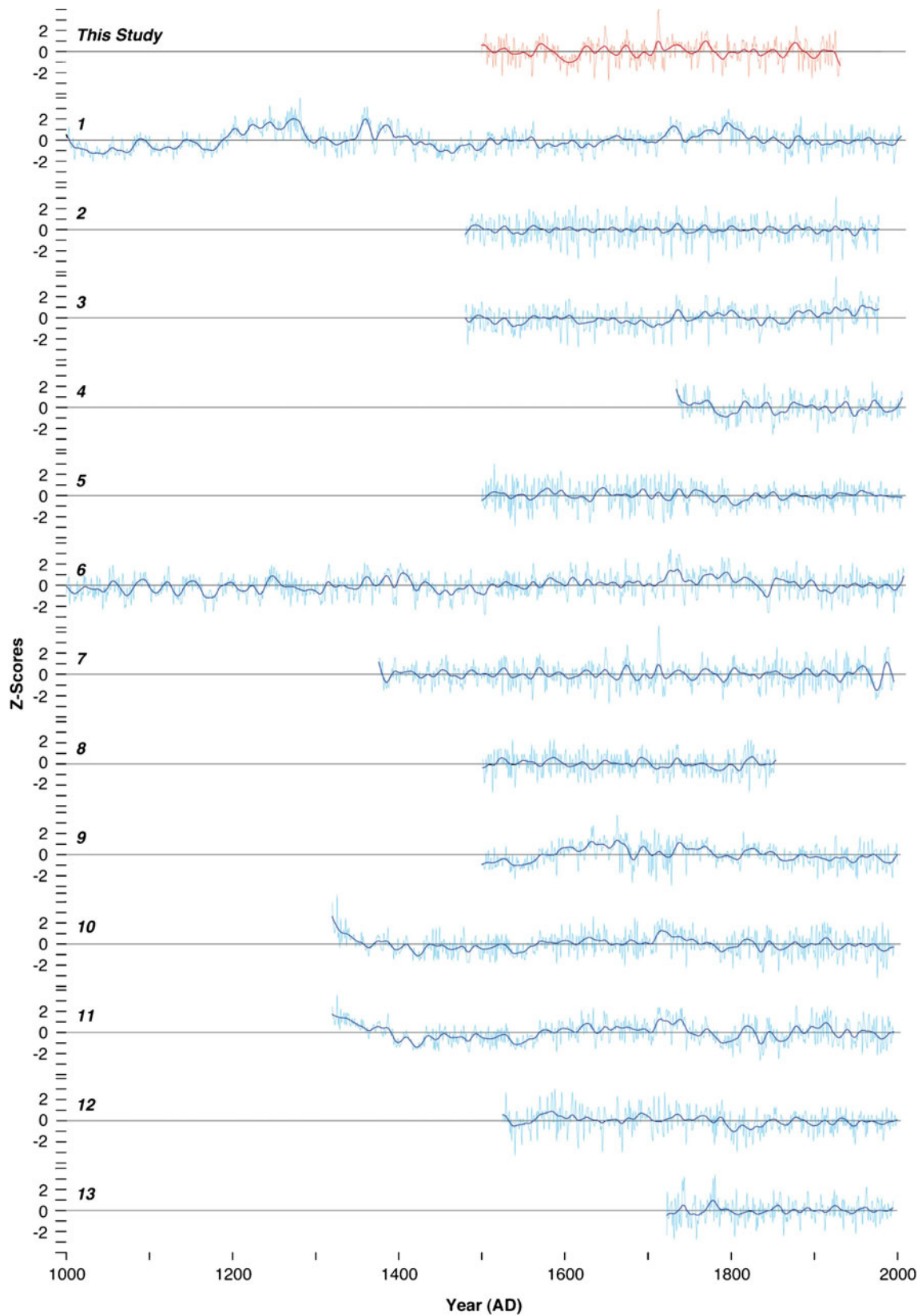


**Fig. 9** Comparison of the Southern Moravian MJ ZIND series with 13 warm-season Central European hydroclimatic proxy-based reconstructions (see Table 2 for details), z-transformed over their individual length, and smoothed with a 20-year spline

grew about one third from 1930 to 1940. The most dramatic increase, however, occurred between 1950 and 1960 when its value doubled. A continuous rise of industrial production was accompanied by significantly increasing air pollution. It must be noted that systematic air pollution measurements at two stations of the Czech Hydrometeorological Institute in Brno started as late as the 1970s (Fig. 8b), making any long-term evaluation impossible. SO<sub>2</sub> concentrations achieved there the highest level in 1985–1987. A pronounced pollution decrease into the 1990s and the onset of the twenty-first century followed peak values in the 1980s.

In this regard, one might also consider the observed mismatch between the TRW-based and instrumental/documentary-based extreme years (Table 1). Several extreme ZIND values reconstructed from TRW were detected for the 1803–1932 period overlapping with the Brno instrumental measurements: in nine cases for negative extremes and in only four for positive extremes. When taking the twentieth century MJ ZIND values from Table 1 as threshold values (i.e., -5.21 and 4.74 correspondingly) for the Brno series (1803–2008), the years of 1806, 1809, 1835, 1863, and 2000 occur as dry extremes, and the years of 1805, 1813, 1843, 1879, 1880, 1910, and 1926 occur as wet extremes. Hence, agreement between reconstructed and measured values occurs only in 1863 (dry), 1879, 1880, and 1926 (wet). Some growth stressors or any ecological factors can be responsible for too narrow TRW that corresponds to changes in ZIND values (e.g., 1898, 1902, or 1929—see Table 1; in 1887, measured ZIND for June was -1.95, but for May 2.26).

The above concert of possible disturbance factors that can impact the growth–climate relationship highlights the

need for careful analysis regarding the temporal stability in the obtained patterns. Novel ensemble approaches to evaluate the likelihood of temporal changes in the hydroclimatic sensitivity of tree-ring chronologies therefore describe a relevant research task. Enhanced studies should consequently consider effects of microclimatology, age-related physiological mechanisms and methodological issues related to standardization and chronology development, and variations in the climatic target data. The occurrence of temporal instability in the relationship between climate forcing and tree growth not only has a substantial effect on biomass productivity rates, with serious implications on carbon sequestration, but also further questions the overall ability of tree ring-based climate reconstructions to capture robustly earlier periods of comparable rates of climate variability, and subsequently to model possible reactions of forest ecosystems in a changing environment.

To range our new reconstruction of MJ ZIND from Southern Moravia in a broader Central European context, 13 different hydroclimatic surrogates were used for comparison (Fig. 9). Data include series based on tree-ring chronologies, documentary indices, instrumental records, and their combination (Table 2). The recent reconstruction shows highest correlations with South Moravian March–July precipitation series based on TRW data by Brázdil et al. (2002) with  $r=0.85$ . Much lower is correlation with the Czech documentary-based MJ ZIND reconstruction ( $r=0.27$ ). Better agreement can be found with an April–August TRW-based precipitation reconstruction for the Vienna Basin ( $r=0.42$ ; Wimmer, personal communication) and a Bavarian TRW-based March–August precipitation

**Table 2** Summary information of 13 annually resolved Central European hydroclimatic series (see Fig. 1a for locations) used for comparison with the herein reconstructed Southern Moravian MJ ZIND

Site	Reference	Period	Lat	Lon	m asl	Region	Season	Lag-1
1	Büntgen et al. 2010c	996–2005	51°11'N	9°12'E	250	C Germany	JJAS	0.62
2	Wilson et al. 2005 (STD)	1480–2001	49°02'N	12°43'E	600	Bavaria	MAMJJA	0.16
3	Wilson et al. 2005 (RCS)	1480–2001	49°02'N	12°43'E	600	Bavaria	MAMJJA	0.38
4	Büntgen et al. 2010a	1734–2006	48°55'N	20°16'E	800	Tatra	JJA	0.43
5	Glaser 2008	1500–2006	48–50°N	8–10°E	300	SW Germany	JJA	0.03
6	Büntgen et al. in prep	-440–2008	47–54°N	4–14°E	350	C Europe	MJ	0.44
7	Brázdil et al. 2002	1376–1996	48°54'N	16°09'E	250	S Moravia	MAMJJA	0.32
8	Dobrovolný et al. in prep	1501–1854	48°54'N	16°09'E	250	S Moravia	MJ	0.03
9	Pauling et al. 2006	1500–2000	48–49°N	20–21°E	250	C Europe	JJA	0.33
10	Wimmer, personal communication	1320–1996	48°12'N	16°22'E	210	Vienna Basin	AMJJA	0.44
11	Wimmer, personal communication	1320–1996	48°12'N	16°22'E	210	Vienna Basin	JJA	0.14
12	Pfister 1999	1525–2000	46–48°N	6–10°E	500	Switzerland	JJA	0.13
13	Oberhuber and Kofler 2002	1724–1997	46°58'N	10°33'E	900	Tyrol	AMJ	0.04

Lat latitude, Lon longitude, m asl altitude, C central, S south, SW southwest

Lag-1 represents the first order autocorrelation coefficient



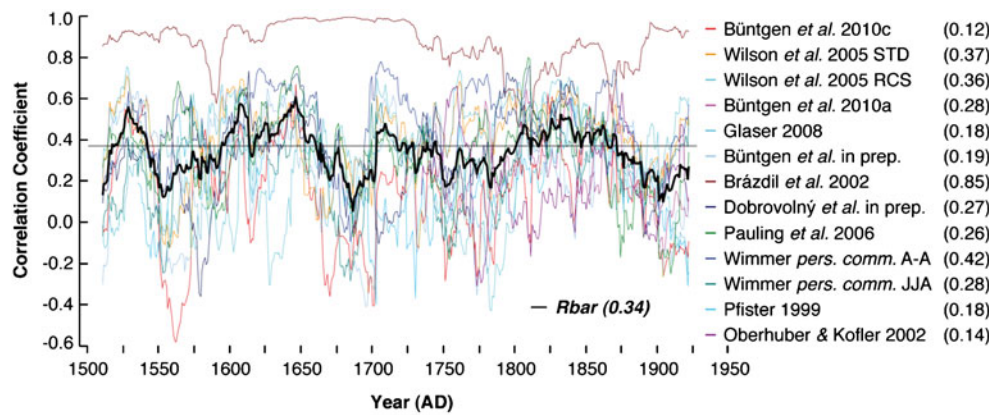


**Fig. 10** Twenty-one-year running correlation coefficients between the TRW-based reconstruction of Southern Moravian MJ ZIND and selected Central European hydroclimatic records (see Fig. 1a for locations and Table 2 for details). The *horizontal line* marks the level

( $r=0.37$ ; Wilson et al. 2005). Running 21-year correlation coefficients among the individual time series are shown in Fig. 10. Averaging these values for the 1500–1932 period ( $R_{bar}$  in Fig. 10), the highest correlations appear around AD 1525, 1600–1650, and 1800–1870. Evaluation of correlations of Central European series with our new Southern Moravian MJ ZIND reconstruction should also consider different hydroclimatic variables (precipitation, ZIND, PDSI) as well as seasonal response differences (Table 2). A slight extension of the short MJ period by surrounding spring and/or summer/autumn months implies a possible bias. The overall low level of explained precipitation/drought variability and its restricted spatial signature further complicate any large-scale comparison (Büntgen et al. 2010b). In fact, the great spatial variability of precipitation regimes related to the occurrence and features of synoptic phenomena causing precipitation or drought cannot be ignored. The spatial signature of precipitation, ZIND, and PDSI indices averaged for Southern Moravia has been expressed via high-resolution correlation

of significant positive correlation at the 0.05 level. *Thick black line* is the mean correlation among all individual series ( $R_{bar}$ ). *Numbers in legend* mark the overall correlation between the Southern Moravian MJ ZIND reconstruction and the corresponding series

fields (Fig. 11). The mean of nine grid-points that represent Southern Moravia was used as core region and correlated against the Central European region that contains the locations of all 13 individual proxy surrogates (Table 2). The area with highest correlations ( $>0.70$ ) extends to a distance of 200–300 km from the core region, with slightly higher correlations and larger distances revealed by the ZIND in comparison to precipitation. Highest correlations are obtained for southeastern Germany, Austria, Bohemia, southern Poland, Slovakia, and Hungary. The prevailing western flow of maritime air masses becomes obvious by the increased longitudinal west–east expansion of positive correlations in comparison to a smaller latitudinal spreading of significant relationships. On the other hand, evidence for a south–north pattern may reflect precipitation influences of Mediterranean cyclones passing into Central Europe along the well-known van Bebbber Vb cyclone track (e.g., van Bebbber 1881), which has also been defined as a major source for flood extremes (e.g., Mudelsee et al. 2004). Our new

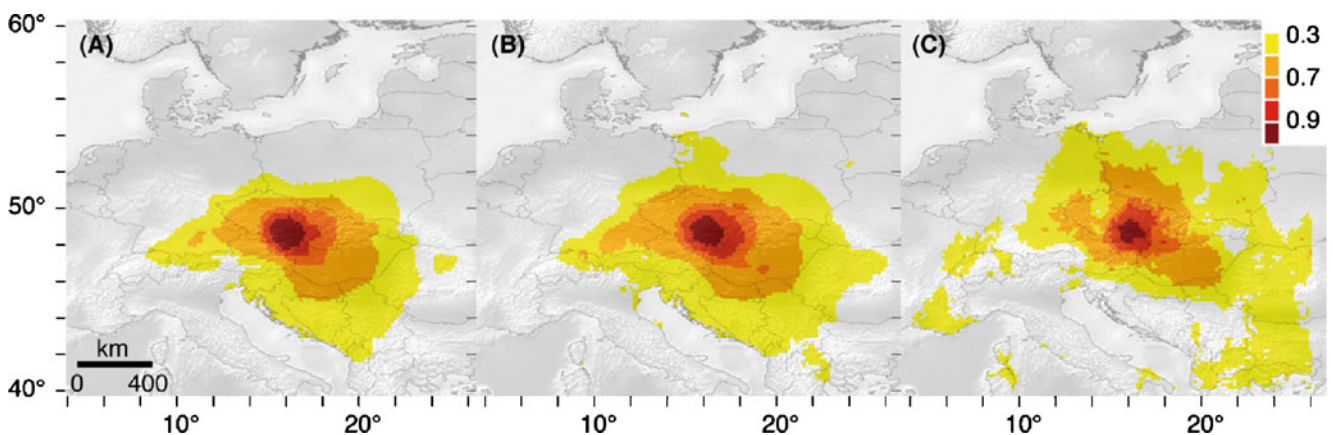


**Fig. 11** Spatial correlation coefficients ( $>0.30$ ) between mean of nine selected grids representing the fir sampling area in Southern Moravia and grids between 4–26°E and 40–58°N (1901–2000): **A** MJ

precipitation totals, **B** MJ ZIND, and **C** PDSI. The  $10' \times 10'$  resolution temperature and precipitation CRU data were used to calculate PDSI and ZIND values

reconstruction of Southern Moravian MJ ZIND shows fairly low spatiotemporal correlations with other series from across the Central European region, which reflects not only the different types of proxy-based hydroclimatic uncertainties but also the great amount of spatial heterogeneity inherent in natural precipitation variability related to local-scale synoptic processes. This picture is in agreement with Brázdil et al. (2010), and it remains difficult to quantify the extent to which some of the longer-term losses of precipitation/drought coherency reflect real spatiotemporal changes of climate variability or nonclimatic reconstruction noise.

In summary, we present a unique collection of 282 living and historic fir TRW series from Southern Moravia (Czech Republic), covering the 1325–2007 period. Growth–climate response analyses between the homogenized station measurements from Brno and a suite of different TRW chronologies are performed over the exceptional 1803–2007 period. Interannual to decadal-scale variations in fir TRW reflect distinct signals of regional-scale precipitation and drought variability. Proxy–target coherency is strongest over the early 1803–1932 interval, but lower coherency is found during the second half of the twentieth century. Our study provides a new and independent Central European TRW-based reconstruction of regional-scale MJ drought variability back to AD 1500, which is accompanied by probabilistic error estimates and shares a significant fraction of documentary-based extreme years from the Czech Lands.

**Acknowledgments** U. Büntgen was supported by the SNF project NCCR-climate (Extract) and the EC project MILLENNIUM (017008), R. Brázdil and P. Dobrovolný by the Grant Agency of the Czech Republic (P209/10/0309), and M. Trnka (521/08/1682). The Czech Hydrometeorological Institute is acknowledged for SO<sub>2</sub> data of the two Brno stations, and two anonymous reviewers for their useful comments.

## References

- Auer I et al (2007) HISTALP—historical instrumental climatological surface time series of the Greater Alpine Region. *Int J Climatol* 27:17–46
- Brázdil R, Štěpánková P, Kyncl T, Kyncl J (2002) Fir tree-ring reconstruction on March–July precipitation in southern Moravia (Czech Republic), 1376–1996. *Clim Res* 20:223–239
- Brázdil R, Pfister C, Wanner H, von Storch H, Luterbacher J (2005) Historical climatology in Europe—the state of the art. *Clim Change* 70:363–430
- Brázdil R, Trnka M, Dobrovolný P, Chromá K, Hlavinka P, Žalud Z (2009) Variability of droughts in the Czech Republic, 1881–2006. *Theor Appl Climatol* 97:297–315
- Brázdil R, Dobrovolný P, Luterbacher J, Moberg A, Pfister C, Wheeler D, Zorita E (2010) European climate of the past 500 years: new challenges for historical climatology. *Clim Change* 101:7–40
- Büntgen U, Esper J, Frank DC, Nicolussi K, Schmidhalter M (2005) A 1052-year tree-ring proxy for Alpine summer temperatures. *Clim Dyn* 25:141–153
- Büntgen U, Frank DC, Wilson R, Carrer M, Urbinati C, Esper J (2008) Testing for tree-ring divergence in the European Alps. *Glob Change Biol* 14:2443–2453
- Büntgen U, Brázdil R, Frank D, Esper J (2010a) Three centuries of Slovakian drought dynamics. *Clim Dyn* 35:315–329
- Büntgen U, Franke J, Frank D, Wilson R, Gonzales-Rouco F, Esper J (2010b) Assessing the spatial signature of European climate reconstructions. *Clim Res* 41:125–130
- Büntgen U, Trouet V, Frank D, Leuschner HH, Friedrichs D, Luterbacher J, Esper J (2010c) Tree-ring indicators of German summer drought over the last millennium. *Quat Sci Rev* 29:1005–1016
- Cook ER, Peters K (1981) The smoothing spline: a new approach to standardizing forest interior tree-ring width series for dendroclimatic studies. *Tree-Ring Bull* 41:45–53
- Cook ER, Peters K (1997) Calculating unbiased tree-ring indices for the study of climatic and environmental change. *Holocene* 7:361–370
- Cook ER, Briffa KR, Meko DM, Graybill DA, Funkhouser G (1995) The ‘segment length curse’ in long tree-ring chronology development for palaeoclimatic studies. *Holocene* 5:229–237
- Cook ER, Seager R, Cane MA, Stahle DW (2007) North American drought: reconstructions, causes, and consequences. *Earth-Sci Rev* 81:93–134
- Dobrovolný P, Brázdil R, Valášek H, Kotyza O, Macková J, Haličková M (2009) A standard palaeoclimatological approach to temperature reconstruction in historical climatology: an example from the Czech Republic, AD 1718–2007. *Int J Climatol* 29:1478–1492
- Dobrovolný P, Moberg A, Brázdil R, Pfister C, Glaser R, Wilson R, van Engelen A, Limanówka D, Kiss A, Haličková M, Macková J, Riemann D, Luterbacher J, Böhm R (2010) Monthly and seasonal temperature reconstructions for Central Europe derived from documentary evidence and instrumental records since AD 1500. *Clim Change* 101:69–107
- Esper J, Cook ER, Krusic PJ, Peters K, Schweingruber FH (2003) Tests of the RCS method for preserving low-frequency variability in long tree-ring chronologies. *Tree-Ring Res* 59:81–98
- Esper J, Frank DC, Büntgen U, Verstege A, Luterbacher J, Xoplaki E (2007) Long-term drought severity variations in Morocco. *Geophys Res Lett* 34:doi:10.1029/2007GL030844
- Frank DC, Büntgen U, Böhm R, Maugeri M, Esper J (2007a) Warmer early instrumental measurements versus colder reconstructed temperatures: shooting at a moving target. *Quat Sci Rev* 26:3298–3310
- Frank D, Esper J, Cook ER, (2007b) Adjustment for proxy number and coherence in a large-scale temperature reconstruction. *Geophys Res Lett* 34:doi:10.1029/2007GL030571
- Friedrichs D, Büntgen U, Esper J, Frank D, Neuwirth B, Löffler J (2009a) Complex climate controls on 20th century oak growth in Central-West Germany. *Tree Physiol* 29:39–51
- Friedrichs D, Trouet V, Büntgen U, Frank DC, Esper J, Neuwirth B, Löffler J (2009b) Species-specific climate sensitivity of tree growth in Central-West Germany. *Trees* 23:729–739
- Glaser R (2008) *Klimageschichte Mitteleuropas. 1200 Jahre Wetter, Klima, Katastrophen*. Wissenschaftliche Buchgesellschaft, Darmstadt, p 264
- Huntington TG (2006) Evidence for intensification of the global water cycle: review and synthesis. *J Hydrol* 319:83–95
- IPCC (2007) *Climate change 2007: the physical science basis*. Contribution of working group I to the fourth assessment report of the IPCC. Cambridge University Press, Cambridge, p 996
- Karl TR (1986) The sensitivity of the Palmer Drought Severity Index and Palmer’s Z index to their calibration coefficients including potential evapotranspiration. *J Climatol Appl Meteorol* 25:77–86
- Mitchell TD, Carter TR, Jones PD, Hulme M, New M (2004) A comprehensive set of high-resolution grids of monthly climate for Europe and the globe: the observed record (1901–2000) and

- 16 scenarios (2001–2100). Technical Report Tyndall Working Paper 55. Tyndall Centre for Climate Change Research, UEA: Norwich
- Moberg A, Sonechkin DM, Holmgren K, Datsenko NM, Karlén W (2005) Highly variable Northern Hemisphere temperatures reconstructed from low- and high-resolution proxy data. *Nature* 433:613–617
- Mudelsee M, Börngen M, Tetzlaff G, Grünewald U (2004) Extreme floods in central Europe over the past 500 years: role of cyclone pathway “Zugstrasse Vb”. *J Geophys Res* 109:D23101
- Oberhuber W, Kofler W (2002) Dendroclimatological spring rainfall reconstruction for an inner Alpine dry valley. *Theor Appl Climatol* 71:97–106
- Palmer WC (1965) Meteorological drought. Office of Climatology Research Paper no. 45, U.S. Weather Bureau. 58 pp
- Pauling A, Luterbacher J, Casty C, Wanner H (2006) Five hundred years of gridded high-resolution precipitation reconstructions over Europe and the connection to large-scale circulation. *Clim Dyn* 26:387–405
- Pfister C, Brázdil R (2006) Social vulnerability to climate in the “Little Ice Age”: an example from Central Europe in the early 1770s. *Clim Past* 2:115–129
- Slonosky VC (2002) Wet winters, dry summers? Three centuries of precipitation data from Paris. *Geophys Res Lett* 29:11–14
- Thornthwaite CW (1948) An approach towards a rational classification of climate. *Geographical Rev* 38:55–94
- Torrence C, Compo GP (1998) A practical guide to wavelet analysis. *Bull Am Meteor Soc* 79:61–78
- van Beber WJ (1881) Die geographische Vertheilung und Bewegung, das Entstehen und Verschwinden der barometrischen Minima in den Jahren 1876 bis 1880. *Zeitschrift der österreichische Gesellschaft für Meteorologie* 16:414–419
- van der Schrier G, Eftymiadis D, Briffa KR, Jones PD (2007) European Alpine moisture variability 1800–2003. *Int J Climatol* 27:415–427
- Vrska T, Adam D, Hort L, Kolar T, Janik D (2009) European beech (*Fagus sylvatica* L.) and silver fir (*Abies alba* Mill.) rotation in the Carpathians—a developmental cycle or a linear trend induced by man? *Forest Ecol Management* 258:347–356
- Wales-Smith GB (1971) Monthly and annual totals of rainfall representative of Kew, Surrey, for 1697 to 1970. *Meteorol Mag* 100:345–362
- Webb RSC, Rosenzweig E, Levine ER (1993) Specifying land surface characteristics in general circulation models: soil profile data set and derived water-holding capacities. *Glob Biogeochem Cycles* 7:97–108
- Wells N, Goddard S, Hayes M (2004) A self-calibrating Palmer drought severity index. *J Climate* 17:2335–2351
- Wigley TML, Briffa KR, Jones PD (1984) On the average of value of correlated time series, with applications in dendroclimatology and hydrometeorology. *J Climatol Appl Meteorol* 23:201–213
- Wilson RJS, Luckman BH, Esper J (2005) A 500 year dendroclimatic reconstruction of spring–summer precipitation from the lower Bavarian Forest region, Germany. *Int J Climatol* 25:611–630